

Science

AAAS

Recycling of Graphite During Himalayan Erosion: A Geological Stabilization of Carbon in the Crust

Valier Galy, *et al.*

Science **322**, 943 (2008);

DOI: 10.1126/science.1161408

The following resources related to this article are available online at www.sciencemag.org (this information is current as of November 6, 2008):

Updated information and services, including high-resolution figures, can be found in the online version of this article at:

<http://www.sciencemag.org/cgi/content/full/322/5903/943>

Supporting Online Material can be found at:

<http://www.sciencemag.org/cgi/content/full/322/5903/943/DC1>

This article **cites 23 articles**, 3 of which can be accessed for free:

<http://www.sciencemag.org/cgi/content/full/322/5903/943#otherarticles>

This article appears in the following **subject collections**:

Atmospheric Science

<http://www.sciencemag.org/cgi/collection/atmos>

Information about obtaining **reprints** of this article or about obtaining **permission to reproduce this article** in whole or in part can be found at:

<http://www.sciencemag.org/about/permissions.dtl>

Recycling of Graphite During Himalayan Erosion: A Geological Stabilization of Carbon in the Crust

Valier Galy,^{1,2*} Olivier Beyssac,³ Christian France-Lanord,² Timothy Eglinton¹

At geological time scales, the role of continental erosion in the organic carbon (OC) cycle is determined by the balance between recent OC burial and petrogenic OC oxidation. Evaluating its net effect on the concentration of carbon dioxide and dioxygen in the atmosphere requires the fate of petrogenic OC to be assessed. Here, we report a multiscale (nanometer to micrometer) structural characterization of petrogenic OC in the Himalayan system. We show that graphitic carbon is preserved and buried in marine sediments, while the less graphitized forms are oxidized during fluvial transport. Radiocarbon dating indicates that 30 to 50% of the carbon initially present in the Himalayan rocks is conserved during the erosion cycle. Graphitization during metamorphism thus stabilizes carbon in the crust over geological time scales.

The burial of organic carbon (OC) in marine sediments represents the second largest sink of atmospheric CO₂ after silicate weathering and subsequent carbonate precipitation (1–4). Rivers play a crucial role in this process by exporting a large flux of OC from the continents to the oceans (5–7), hence generating a long-term C sink. OC exported by rivers is, however, a mix of (i) “recent” OC (OC_{recent}) derived from plant detritus, associated soil organic matter, and autotrophic carbon production by aquatic plants, and (ii) petrogenic OC (OC_{petro}) derived from erosion of carbonaceous rocks [e.g., (8–11)]. Burial of the latter is a simple recycling of reduced C and has no effect on the long-term atmospheric CO₂ and O₂ levels. Conversely, its oxidation consumes O₂ from and returns CO₂ to the atmosphere, thereby counteracting the effect of OC_{recent} burial. Addressing the role of continental erosion on the global C cycle thus requires assessing the fate of OC_{petro} during erosion and fluvial transport.

The Himalayan range undergoes an intense physical erosion producing an enormous flux of sediment (~2 billion tons per year) carried by the Ganges-Brahmaputra (G-B) fluvial system to the Bengal Fan turbiditic system [e.g., (12)]. Recently, we showed that OC is very efficiently buried in sediments of the Bengal Fan (13). This contrasts with most large deltaic systems, including the Amazon (5–7). We estimated that Himalayan erosion is responsible for ~10 to 20% of the global burial of OC_{recent}, implying a global impact on the OC cycle. The Himalayan example illustrates the importance of active origins in the global C cycle and therefore offers an ideal case study to determine the fate of OC_{petro} during continental erosion.

Several methods have been developed to detect and quantify the most refractory pool of C in rocks, river sediments, and marine sediments, often referred to as black carbon [e.g., (14–17)]. The selectivity of these methods is, however, based on

the refractory character of the C particles, which is not unique to OC_{petro}, but also characterizes some soil OC (charcoals) or anthropic C (e.g., soots). Consequently, they isolate a much larger pool of C and thus overestimate the petrogenic component. Here, we combine Raman microspectroscopy (RM) and transmission electron microscopy (TEM) to (i) detect OC_{petro} in river and marine sediments and (ii) characterize its multiscale structural organization (nm to μm). RM allows in situ analysis, preserving the textural information of OC (particle size and shape) itself, but also its relations with minerals (aggregates and inclusions). Combining 002 lattice-fringes imaging and electron diffraction, TEM gives an insight into the nm-scale structure of the aromatic skeleton composing OC_{petro} (16, 17). Finally, we use radiocarbon dating of bulk acid-insoluble OC to quantify the proportion of OC_{petro} and OC_{recent} in river sediments (17).

We have analyzed a sample set covering the whole erosional and depositional system, including Himalayan source rocks, G-B river sediments, and Bengal Fan sediments (tables S1 and S2). To study the fate of OC_{petro} during fluvial transport, river

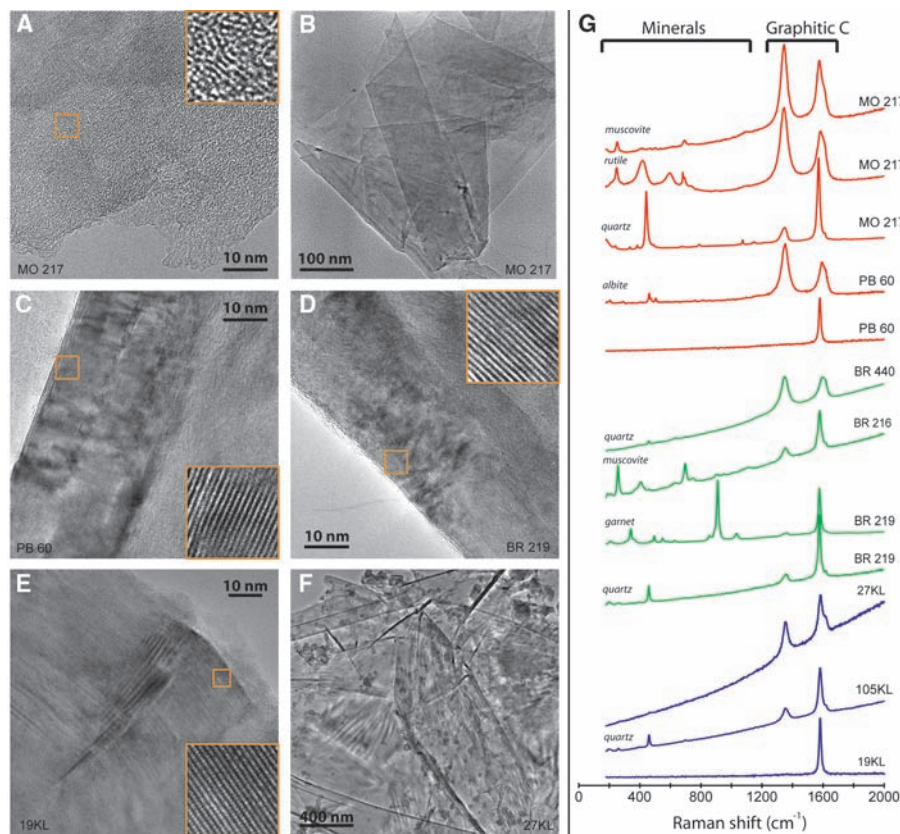


Fig. 1. RM and TEM characterization of OC_{petro} in riverine and marine sediments. (A) Image of 002 lattice-fringes (002LF) of disordered and microporous OC_{petro} in Narayani bed load. (B) Image (002LF) of graphitic C in Narayani bed load. (C) Low-magnification (LM) image of a graphite particle in Narayani suspended load. (D) Image (002LF) of graphitic OC_{petro} in Lower Meghna bed load. (E) Image (002LF) of graphitic OC_{petro} in distal Bengal Fan sediment. (F) LM image of graphite particles in distal Bengal Fan sediment. In (A), (C), (D), and (E), the orange inset is a zoom (5-nm side) located on the main image. (G) Selection of representative Raman spectra from Himalayan rivers (red), Lower Meghna (green), and Bengal Fan sediments (blue). These spectra were obtained from both individual OC_{petro} particles (no mineral contribution in the spectrum) and OC_{petro} inclusions/aggregates within minerals (mineral contribution in the spectrum as depicted).

¹Woods Hole Oceanographic Institution, Department of Marine Chemistry and Geochemistry, Woods Hole, MA 02543, USA.

²Centre de Recherches Pétrographique et Géochimiques, CNRS, Institut National des Sciences de l'Univers (INSU), Nancy Université, BP 20, 54501 Vandœuvre-lès-Nancy, France.

³Laboratoire de Géologie, Ecole Normale Supérieure, CNRS-UMR 8538, 24 Rue Lhomond, F-75005 Paris Cedex 5, France.

*To whom correspondence should be addressed. E-mail: vgal@whoi.edu

sediments were collected from the Himalayan range to the Bangladesh delta (fig. S1). In the G-B system, suspended and bed sediments define a continuum from fine, clay-rich, surface-suspended sediments to coarse, quartz-rich, bed sediments. OC content increases with decreasing grain size and increasing proportions of phyllosilicates (18). To take this variability into account, we analyzed OC in suspended sediments collected along depth profiles within the river as well as from dredged riverbed sediments. To describe the Bengal Fan turbiditic system, we used sediments drilled by the research vessel (RV) Sonne cruise 93 (19) in the shelf, the middle fan channel levee system, and the deep fan (fig. S2).

OC_{petro} has been detected by RM and TEM in all investigated sediments, including the most distal regions of the Bengal Fan (Fig. 1). Using RM, OC_{petro} was identified in various forms: (i) discrete “free” particles from a few to several tens of μm size; (ii) inclusions within quartz, calcite, and metamorphic minerals; and (iii) aggregates with minerals, mostly micas. The latter two have an obvious petrogenic origin, whereas in the former the most disordered C may be OC_{recent} (soot or charcoal) or OC_{petro} from very low-grade metamorphic rocks (17).

RM shows a large structural variety of OC_{petro} in bed and suspended loads from Himalayan rivers (Fig. 1). This is confirmed by TEM investigations that reveal the presence of turbostratic disordered OC_{petro} to perfectly crystalline graphite in these samples. The structural variety of OC_{petro} reflects the zoning of metamorphism in the source rocks of the Himalayan range [e.g., (20)], from low- to high-grade metamorphism (fig. S1). Similar structural variety is observed within the vertical depth profiles collected at the outflow of the range and in Bangladesh, although the less-ordered OC_{petro} is rarely observed. In all marine sediments, both RM and TEM investigations show that OC_{petro} detected by these methods is almost exclusively highly ordered polycrystalline or pristine graphite (Fig. 1) and that disordered OC_{petro} is rare (17). Because we do not observe any segregation in terms of crystallinity of OC_{petro} along vertical depth profiles in rivers, we posit that OC_{petro} is homogeneously transported as a continuum through the river section. However, oxidation of the less-graphitic OC_{petro} occurs within the Himalayan range and during the floodplain transit, because these forms are virtually absent in the Bengal Fan sediments, which is consistent with OC_{recent} oxidation and replacement documented in the Gangetic floodplain (18). Such selective oxidation might be related to the higher chemical reactivity due to the presence of atoms other than C (primarily H and O) and enhanced by the high nano- to micro-porosity of disordered OC_{petro} compared with graphite.

Estimating the proportion of OC contained in the Himalayan rocks that is ultimately oxidized during the erosion cycle requires quantifying the amount of OC_{petro} in the sediments exported by G-B rivers. We measured the ¹⁴C composition of bulk acid-insoluble OC (expressed as the fraction

of modern C, Fm) in sediments collected along depth profiles. OC_{petro} is radiocarbon free (Fm = 0), whereas OC_{recent} has variable amounts of radiocarbon (Fm > 0) depending on its residence time in the basin. In the Himalayan basin, a consequence of intense physical erosion is that none of the OC_{recent} particles contained in soils is radiocarbon free, which gives to OC_{petro} a unique geochemical signature (Fm = 0).

The results are presented in Fig. 2 as modern OC content (Fm × %OC) plotted as a function of the total OC content (see also fig. S4 and table S1). Sediments collected along depth profiles define

linear trends in this diagram. Suspended and bed sediments from each depth profile thus have identical amount of OC_{petro} (17). This consistency derives from the generation of sediment continuums by mixing processes during fluvial transport. A statistical analysis of the trends drawn in Fig. 2 allows the determination of the amount of OC_{petro} (17). Large trans-Himalayan rivers sampled at the outflow of the range appear to carry variable amounts of OC_{petro}. We estimate an OC_{petro} content of 0.05% and 0.03% for the Narayani and Kosi, respectively. This variability likely derives from intrinsic characteristics of the

Fig. 2. (Top) Modern OC content (Fm × %OC) of sediments collected over depth profiles in rivers from the G-B system as a function of their total OC content. In this representation, sediments with similar amount of OC_{petro} define linear trends, whose intercept with the x axis gives %OC_{petro} (17). Each solid line represents the best linear fit defined by sediments from the same depth profile. Himalayan rivers sediments (green, Narayani; yellow, Kosi) have variable amounts of OC_{petro}, whereas Ganges (blue) and Brahmaputra (red) in Bangladesh have similar amounts of OC_{petro} around an average value of 0.025%. Radiocarbon composition of Bengal Fan sediments (hexagons) is comparable with that of river sediments, indicating they have similar content of OC_{petro}. **(Bottom)** Total OC content of Himalayan source rocks (black, High-Himalayan Crystalline; light gray, Lesser Himalaya; dark gray, composite gravel samples) from (13). The average OC content of source rocks ranges between 0.05 and 0.08%.

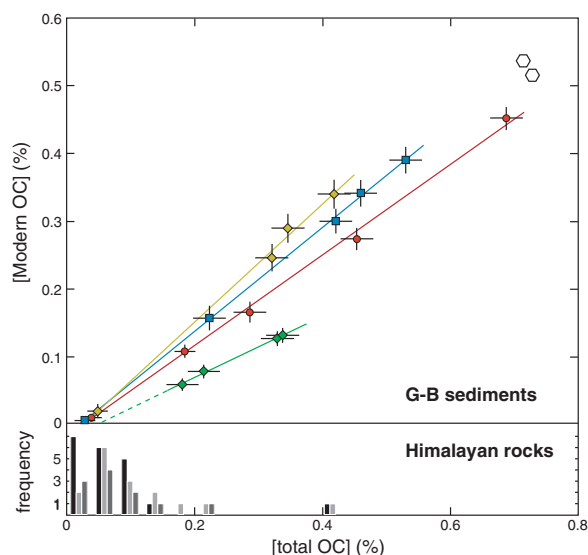
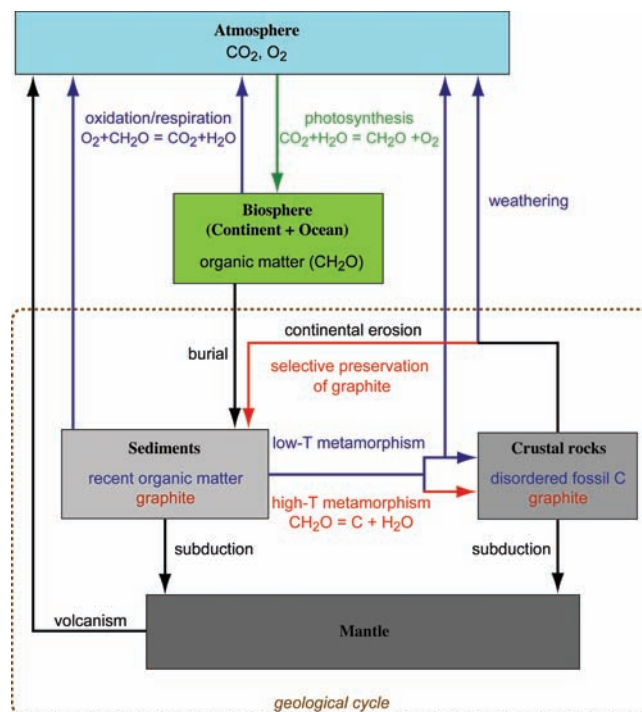


Fig. 3. A model of the long-term OC cycle highlighting the role of graphitization. The graphite formed during high-temperature (>500°C) metamorphism is preserved during continental erosion and returns to the atmosphere only throughout volcanism. Graphitization thus stabilizes reduced C, confining it to a geological subcycle and maintaining an imbalance between photosynthesis and respiration/oxidation over geological time scales.



drainage basins. Our data consistently indicate an OC_{petro} content of 0.02 to 0.03% in the sediments exported by the Brahmaputra and the Ganges sampled close to their mouths in the Bangladesh delta. We therefore estimate that sediments delivered to the Bay of Bengal contain $\sim 0.025\%$ of OC_{petro} derived from the erosion of Himalayan rocks. Because the oxidation of OC in the marine system before deposition in the Bengal Fan is negligible (13), the OC_{petro} content of these sediments must be comparable to that of the sediments exported by G-B rivers. Moreover, for two sediments deposited in the channel-levee system of the Bengal Fan, we corrected the ^{14}C composition of OC for their respective deposition age determined by ^{14}C dating of foraminifera (21). Their position in Fig. 2 is highly consistent with sediments delivered by G-B rivers, indicating that they have similar content of OC_{petro} . Consequently, we estimate that Bengal Fan sediments contain $\sim 0.025\%$ of OC_{petro} . To evaluate the fate of petrogenic OC during the Himalayan erosion cycle, this value must be compared to the mean OC content of Himalayan rocks. The latter has been estimated to be 0.05 to 0.08%, on the basis of individual rock samples and composite gravels extracted from the bed of Himalayan rivers (13, 22, 23). Based on these figures, at least 30% (40 ± 10) of the OC contained in the Himalayan rocks appears to be preserved and recycled during the erosion cycle, mostly through burial of highly graphitic carbon in the Bengal Fan sediments. In turn, the oxidative flux of OC_{petro} associated with Himalayan erosion is estimated to be $0.67 (\pm 0.25) \times 10^{11}$ mol/year, which is comparable to the long-term CO_2 consumption by silicate weathering (0.6×10^{11} mol/year (24)) but one order of magnitude lower than the CO_2 consumption by OC_{recent} burial in the Bengal Fan [$3.1 (\pm 0.3) \times 10^{11}$ mol/year (13)].

The Himalayan example highlights the role of mountain building in the long-term stabilization of Earth climate and atmospheric composition. Active orogenesis not only promotes CO_2 consumption by both silicate weathering and terrestrial organic carbon burial but also stabilizes C in the crust over geological time scales through graphitization of OC (Fig. 3). Metamorphism during orogenesis actually transforms labile photosynthetic C into refractory petrogenic C through graphitization, the efficiency of this transformation being mainly controlled by the metamorphic temperature. The selective preservation of graphite during erosion and weathering indicates that graphitization occurring during metamorphism subtracts C from the external cycle (atmosphere-biosphere-ocean) and locks it into the geological cycle (Fig. 3). Mechanisms capable of returning graphitic C into the atmosphere involve subduction and volcanism, both having a very long characteristic time compared with surface processes. At geological time scales, the graphitization thus maintains an imbalance between photosynthesis and respiration by locking reduced C into the crust, hence promoting both consumption of CO_2 and accumulation of O_2 in the atmosphere.

References and Notes

1. R. A. Berner, *Science* **249**, 1382 (1990).
2. J. M. Hayes, J. R. Waldbauer, *Phil. Trans. R. Soc. London B Biol. Sci.* **361**, 931 (2006).
3. R. M. Garrels, A. Lerman, F. T. Mackenzie, *Am. Sci.* **64**, 306 (1976).
4. A. C. Lasaga, R. A. Berner, R. M. Garrels, in *The Carbon Cycle and Atmospheric CO_2 : Natural Variations Archean to Present*, E. T. Sundquist, W. S. Broecker, Eds. (American Geophysical Union, Washington, 1985), vol. 32, pp. 397–411.
5. D. J. Burdige, *Global Biogeochem. Cycles* **19**, GB4011 (2005).
6. J. I. Hedges, R. G. Keil, R. Benner, *Org. Geochem.* **27**, 195 (1997).
7. B. Schlünz, R. R. Schneider, *Int. J. Earth Sci.* **88**, 599 (2000).

8. N. E. Blair *et al.*, *Geochim. Cosmochim. Acta* **67**, 63 (2003).
9. W. M. Sackett, C. W. Poag, B. J. Eadie, *Science* **185**, 1045 (1974).
10. N. E. Blair, E. L. Leithold, R. C. Aller, *Mar. Chem.* **92**, 141 (2004).
11. A. F. Dickens, Y. Gélinas, C. A. Masiello, S. Wakeham, J. I. Hedges, *Nature* **427**, 336 (2004).
12. A. Galy, C. France-Lanord, *Geology* **29**, 23 (2001).
13. V. Galy *et al.*, *Nature* **450**, 407 (2007).
14. Y. Gélinas, K. M. Prentice, J. A. Baldock, J. I. Hedges, *Environ. Sci. Technol.* **35**, 3519 (2001).
15. P. R. Haberstroh *et al.*, *Geochim. Cosmochim. Acta* **70**, 1483 (2006).
16. C. A. Masiello, *Mar. Chem.* **92**, 201 (2004).
17. Materials and methods are available as supporting material on Science Online.
18. V. Galy, C. France-Lanord, B. Lartiges, *Geochim. Cosmochim. Acta* **72**, 1767 (2008).
19. V. Ittekkot, H. R. Kudrass, D. Quadfasel, D. Unger, *Deep Sea Res. Part II Top. Stud. Oceanogr.* **50**, 853 (2003).
20. O. Beyssac, L. Bollinger, J.-P. Avouac, B. Goffe, *Earth Planet. Sci. Lett.* **225**, 233 (2004).
21. V. Galy *et al.*, *Quat. Sci. Rev.* **27**, 1396 (2008).
22. A.-M. Aucour, C. France-Lanord, K. Pedoja, A.-C. Pierson-Wickmann, S. M. F. Sheppard, *Global Biogeochem. Cycles* **20**, GB2006 (2006).
23. C. France-Lanord, L. A. Derry, *Nature* **390**, 65 (1997).
24. A. Galy, C. France-Lanord, *Chem. Geol.* **159**, 31 (1999).
25. We thank H. Kudrass, who provided Bengal Fan samples collected during the RV Sonne cruise; M. Rahman from Dhaka University; A. Gajurel from Tribhuvan University (Kathmandu) for their help during field work in Bangladesh and Nepal; and A. Galy for insightful comments, as well as J. Hayes and an anonymous referee for constructive reviews. This study was supported by the French INSU program "Reliefs de la Terre" and a scholarship from Woods Hole Oceanographic Institution to V.G.

Supporting Online Material

www.sciencemag.org/cgi/content/full/322/5903/943/DC1
Material and Methods
SOM Text
Figs. S1 to S4
Tables S1 and S2
References

5 June 2008; accepted 2 October 2008
10.1126/science.1161408

Induced Pluripotent Stem Cells Generated Without Viral Integration

Matthias Stadtfeld,^{1,2,4,5} Masaki Nagaya,^{3,5} Jochen Utikal,^{1,2,4,5} Gordon Weir,^{3,5} Konrad Hochedlinger^{1,2,4,5*}

Pluripotent stem cells have been generated from mouse and human somatic cells by viral expression of the transcription factors Oct4, Sox2, Klf4, and c-Myc. A major limitation of this technology is the use of potentially harmful genome-integrating viruses. We generated mouse induced pluripotent stem (iPS) cells from fibroblasts and liver cells by using nonintegrating adenoviruses transiently expressing Oct4, Sox2, Klf4, and c-Myc. These adenoviral iPS (adeno-iPS) cells show DNA demethylation characteristic of reprogrammed cells, express endogenous pluripotency genes, form teratomas, and contribute to multiple tissues, including the germ line, in chimeric mice. Our results provide strong evidence that insertional mutagenesis is not required for in vitro reprogramming. Adenoviral reprogramming may provide an improved method for generating and studying patient-specific stem cells and for comparing embryonic stem cells and iPS cells.

The introduction of defined transcription factors into mouse and human somatic cells has recently been shown to reprogram the developmental state of mature cells into that of pluripotent embryonic cells, generating

so-called "induced pluripotent stem (iPS) cells" (1). iPS cells have been generated from multiple cell types by viral expression of Oct4 and Sox2, combined with either Klf4 and c-Myc (1–11) or LIN28 and Nanog (12). iPS cells are molecularly

and functionally highly similar to ES cells, which makes in vitro reprogramming an attractive approach to produce patient-specific stem cells for studying and potentially treating degenerative disease. Indeed, reprogrammed skin cells have recently been shown to alleviate the symptoms of Parkinson's disease (13) and sickle cell anemia (14) in mouse models. However, a major limitation of this technology is the use of viruses that integrate into the genome and are associated with the risk of tumor formation due to the spontaneous reactivation of the viral transgenes (8). The low efficiency of reprogramming (0.01 to 0.1% of input cells) also raised the possibility that insertional mutagenesis may be a prerequisite for in vitro reprogramming (15). For example, the retroviral tagging of explanted hematopoietic stem cells has been previously shown to select for clones in which the retroviral construct had inserted proximal to self-renewal genes and thus causes their activation (16). Whereas the sequencing of a limited number of insertion sites in iPS cells did not reveal common targets (17), this possibility has not been unequivocally ruled out yet (15).